Effects of Molybdenum Doping on the Layered $Li[Ni_{0.5+x}Mn_{0.5-2x}Mo_x]O_2$ Cathode Materials for Lithium Secondary Batteries

Sang Ho Park, Sung Woo Oh, Sung Goon Kang,[†] Seung-TaeK Myung,[††] and Yang-Kook Sun*
Department of Chemical Engineering, Hanyang University, Seoul 133-791, Korea
[†]*Division of Material Science and Engineering, Hanyang University, Seoul 133-791, Korea*
[††]*Department of Chemical Engineering, Faculty of Engineering, Iwate University, 4-3-5 Ueda, Morioka, Iwate 020-8551*

(Received September 8, 2003; CL-030835)

Molybdenum-doped layered $Li[Ni_{0.5+x}Mn_{0.5-2x}Mo_x]O_2$ materials were synthesized by an ultrasonic spray pyrolysis method. Single phase of $Li[Ni_{0.5+x}Mn_{0.5-2x}Mo_x]O_2$ could be prepared in $0 \leq x \leq 0.05$ region. Structural and electrochemical properties of the $Li[Ni_{0.5+x}Mn_{0.5-2x}Mo_x]O_2$ were characterized by means of X-ray diffraction, Rietveld refinements, and galvanostatic charge/discharge test. The discharge capacity increased linearly with the increase of molybdenum contents, x, and exhibited a high discharge capacity over 175 mAh/g between 2.8 and 4.4 V with a good capacity retention.

Layered lithiated transition metal oxides such as $LiCoO_2$, $LiNiO_2$, and $LiMnO_2$ are of great interest for use in the application of lithium rechargeable batteries as positive electrode materials.[1–3] The commercialized $LiCoO_2$ still have disadvantages of high cost and toxicity. $LiNiO_2$ and $LiMnO_2$ have been extensively studied as possible alternatives to $LiCoO_2$. However, $LiNiO_2$ is well known that it is difficult to synthesize in its stoichiometric form and further, delithiated Li_xNiO_2 has poor thermal stability.[4] $LiMnO_2$ was observed to undergo a phase transformation to a spinel-like phase during cycling because of a thermodynamic instablility of the layered structure, causing two voltage plateaus on 3 and 4 V.[5,6]

Recently, Ohzuku et al.[7] and Lu et al.[8] have proposed a concept of a solid solution with $LiNiO_2$ and $LiMnO_2$. $Li[Ni_{0.5}Mn_{0.5}]O_2$ is an attractive cathode material for lithium secondary batteries. Kim et al.[9] reported on the $(1-x)Li_2TiO_3{\cdot}xLiNi_{0.5}Mn_{0.5}O_2$ system, in which partially substituted Li_2TiO_3 oxide stabilizes cycling performance of $LiNi_{0.5}Mn_{0.5}O_2$ electrode. Kang et al.[10] reported the $Li[Ni_{0.5-x}Mn_{0.5-x}M_{2x}]O_2$ (M = Mg, Al, Co, Ni, Ti; $x = 0$, 0.025) materials. Y. Arachi et al.[11] reported that Ni^{2+} and Mn^{4+} coexist in the layered $Li[Ni_{1/2}Mn_{1/2}]O_2$ material and Ni^{2+} ion is oxidized to Ni^{3+}, while Mn^{4+} ions remain mostly unchanged as 0.5Li is deintercalated from the material. The stable cycling behavior of the $Li[Ni_{1/2}Mn_{1/2}]O_2$ material might be attributed to the stable tetravalent oxidation state of Mn during electrochemical cycling. However, $Li[Ni_{1/2}Mn_{1/2}]O_2$ and their derivative delivered a low reversible capacity of 150 mAh/g in the voltage range of 2.8 to 4.3 V comparing with $LiNiO_2$ layered material. From these previous reports, it is thought that the content of Ni is fixed to 0.5. Here, if the amount of Ni can be greater than 0.5 in $Li[Ni_{0.5}Mn_{0.5}]O_2$, it is able to expect that the obtainable capacity would be higher because the electro active amount of Ni^{II} increases.

Recently, we reported on the synthesis and electrochemical properties of $Li[Ni_{1/2}Mn_{1/2}]O_2$ powder prepared by an ultrasonic spray pyrolysis method.[12] The ultrasonic spray pyrolysis is an effective synthetic technique having advantages such as a good stoichiometric control, homogeneous precursor, short production time, and spherical morphology. In this study, we have attempted to synthesize Mo^{VI} ion-doped $Li[Ni_{0.5+x}Mn_{0.5-2x}Mo_x]O_2$ (x in 0, 0.01, 0.02, and 0.05) materials using MoO_3 as a dopant. The structural and electrochemical properties of the prepared materials were characterized.

$Li[Ni_{0.5+x}Mn_{0.5-2x}Mo_x]O_2$ ($x = 0$, 0.01, 0.02, 0.05) powders were prepared as follows: $[Ni_{0.5+x}Mn_{0.5-2x}Mo_x]O_2$ precursor was first synthesized using the spray pyrolysis method. Stoichiometric amounts of $Ni(NO_3){\cdot}6H_2O$ (Aldrich) and $Mn(NO_3)_2{\cdot}4H_2O$ (Sigma) were dissolved in distilled water, and MoO_3 (Merck) was dissolved in NH_4OH solution. Then, the aqueous solution was added into a continuously agitated aqueous citric acid solution. The molar concentration of citric acid was fixed in 0.2 M. The starting solution was atomized using an ultrasonic nebulizer with a resonant frequency of 1.7 MHz. The aerosol stream was introduced into the vertical quartz reactor heated at 500 °C. The flow rate of air used as a carrier gas was 10 L/min. The prepared powder was thoroughly mixed with $LiOH{\cdot}H_2O$. After the mixture was softly ground, these were heated again at 900 °C in a box furnace with a heating rate of 1 °C/min.

The powder X-ray diffraction (XRD, Rint-2000, Rigaku, Japan) measurement using Cu Kα radiation was employed to identify the crystalline phase of the synthesized material. Rietveld refinement of the collected data was made using the FULLPROF Rietveld program.[13] Galvanostatic charge/discharge cycling was performed in a 2032-type coin cell. For the fabrication of the positive electrode, 20 mg of $Li[Ni_{0.5+x}Mn_{0.5-2x}Mo_x]O_2$ was mixed with 12 mg of conductive binder (8 mg of TAB and 4 mg of graphite). The mixture was pressed on 200 mm^2 stainless steel mesh used as the current collector and dried at 140 °C for 10 h in a vacuum oven. The test cell was made of a cathode and a lithium metal anode (Cyprus Foote Mineral Co.) separated by a porous polypropylene film (Celgard 3401). The electrolyte solution was 1 M $LiPF_6$ in a mixture of ethylene carbonate (EC) and diethyl carbonate (DEC) in a 1:1 volume ratio. The cell was assembled in an argon-filled glove box. The charge/discharge measurements were carried out between 2.8 and 4.4, 4.5, 4.6, 4.7 V potential ranges at a current density of 0.2 mA/cm^2 (20 mA/g).

Figure 1 shows XRD spectra for $Li[Ni_{0.5+x}Mn_{0.5-2x}Mo_x]O_2$ ($0 < x < 0.05$) powders. All samples can be indexed based on a hexagonal α-$NaFeO_2$ structure with a space group of $R\bar{3}m$. No impurity-related peaks are observed from the XRD pattern with in-

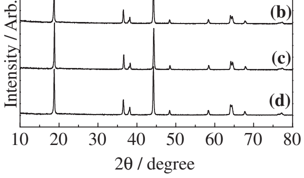

Figure 1. X-ray diffraction patterns for $Li[Ni_{0.5+x}Mn_{0.5-2x}Mo_x]O_2$ powders, x in (a) 0, (b) 0.01, (b) 0.02, and (c) 0.05.

Table 1. Crystallographic data of the Li[$Ni_{0.5-x}Mn_{0.5-2x}Mo_x$]$O_2$ powders

Initial composition	a (Å)	c (Å)	c/a	I_{003}/I_{104}	R_{wp} (%)	R_{Bragg}-factor (%)
Li[$Ni_{0.5}Mn_{0.5}$]O_2	2.87	14.26	4.96	1.45	11.2	1.62
Li[$Ni_{0.51}Mn_{0.48}Mo_{0.01}$]$O_2$	2.88	14.30	4.95	1.19	9.47	2.10
Li[$Ni_{0.52}Mn_{0.46}Mo_{0.02}$]$O_2$	2.89	14.31	4.95	1.11	7.39	2.17
Li[$Ni_{0.55}Mn_{0.40}Mo_{0.05}$]$O_2$	2.90	14.32	4.94	0.95	7.87	2.03

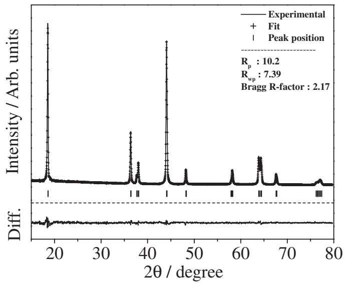

Figure 2. Rietveld refinement pattern of Li[$Ni_{0.52}Mn_{0.46}Mo_{0.02}$]$O_2$ powders.

creasing Mo doping contents. Therefore, all the XRD patterns were able to be indexed as a typical layered structure without any impurity phase, which is ascribed to the homogeneous atomic scale mixing of the precursor. The clear splitting of the reflections assigned to the Miller indices (006, 102) and (108, 110) is characteristic of the layered structure. The lattice constants, a and c, c/a ratio, and I_{003}/I_{104} of the hexagonal unit cell of the increasing Mo content samples are shown in Table 1. As the Mo content increases, the lattice constants a and c increase from 2.87 to 2.90 Å, and 14.26 to 14.32 Å, respectively. Larger ionic size of Mo^{6+} (0.59 Å) and Ni^{2+} (0.69 Å) than that of Mn^{+4} (0.53 Å) might cause the increase in lattice parameters. Besides, the integrated intensity ratio of the I_{003}/I_{104} peaks decreases from 1.45 to 0.95. These results indicate that some cation mixing whereby a fraction of Ni and Li ions interchange sites in the crystal lattice.

The Rietveld refinement analysis with X-ray diffraction (XRD) pattern was given in Figure 2. Rietveld refinement analysis was based on O3 hexagonal structure (S.G. $R\bar{3}m$, No. 166). Refinement profiles for this material indicated that all the peaks fits well to the space group of $R\bar{3}m$, showing the R_{wp} of 7.39%. Therefore, we considered that Li[$Ni_{0.52}Mn_{0.46}Mo_{0.02}$]$O_2$ material in this study has that the crystal structure is the $O3$ hexagonal structure with a space group of $R\bar{3}m$ (No. 166). The refinement result shows that a small amount of Ni(0.074(3)) occupied the Li (3b) site and the corresponding amount of Li(0.090(5)) was located at the Ni (3a) site, respectively. Furthermore, c/a ratios are over 4.93, indicating the formation of well-developed hexagonal phase at all Mo doping contents ($x \leq 0.05$).

Figure 3a shows specific discharge capacity vs number of cycle for Li/Li[$Ni_{0.5+x}Mn_{0.5-2x}Mo_x$]$O_2$ ($x = 0$–0.05) cell at room temperature at a constant current density of 0.2 mA/cm^2 (1/8C rate). Li/Li[$Ni_{0.5}Mn_{0.5}$]O_2 cell delivered an initial discharge capacity of 167 mAh/g. However, molybdenum-doped samples showed higher capacity than undoped electrode, with good capacity retention. As it was suggested that if the electroactive Ni amount increases the resulting capacity would increase, the doped sample clearly exhibited enhanced capacity during cycling. Because Li[$Ni^{II}_{0.5+x}Mn^{IV}_{0.5-2x}Mo^{VI}_x$]$O_2$ material allows Li^+ ions to be extracted more. Therefore, Mo-doped sample could be delivered higher discharge capacity than undoped sample. Figure 3b shows the charge/discharge curves and specific discharge capacities for the Li/Li[$Ni_{0.52}Mn_{0.46}Mo_{0.02}$]$O_2$ cell as a function of various cut-off voltage between 2.8 and 4.4, 4.5, 4.6, 4.7 V. The discharge capacities increased linearly with the upper cut-off voltage limit higher. In the voltage range of 2.8–4.4, 4.5, 4.6, and 4.7, the discharge capacities of the Li[$Ni_{0.52}Mn_{0.46}Mo_{0.02}$]$O_2$ electrodes were 177, 187, 195, and 200 mAh/g, respectively, and these cells show still excellent cyclabilities. The voltage profiles showed very smooth and monotonous curves, even though the upper cut-off voltage was as high as 4.7 V. Figure 4 shows differential capacity vs voltage of the 5th, 25th, 50th cycles for the Li/Li[$Ni_{0.52}Mn_{0.46}Mo_{0.02}$]$O_2$ cell. From the redox peak, it can be denoted that structural change did not occurred during the repetitive lithium extraction/insertion process. Therefore, it is concluded that Mo doping in Li[$Ni_{0.5}Mn_{0.5}$]O_2 is effective to enhance obtainable capacity as well as cyclability substantially even in higher voltage cycling.

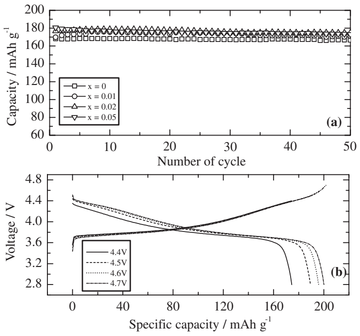

Figure 3. (a) Capacity vs number of cycle for Li/Li[$Ni_{0.5+x}Mn_{0.5-2x}Mo_x$]$O_2$, (b) Voltage curves vs specific capacity of Li/Li[$Ni_{0.52}Mn_{0.46}Mo_{0.02}$]$O_2$.

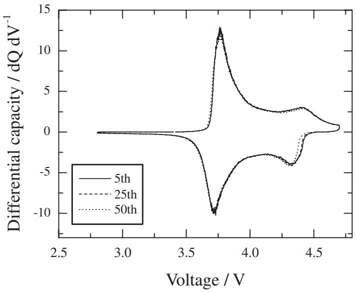

Figure 4. Differential capacity vs voltage of Li/Li[$Ni_{0.52}Mn_{0.46}Mo_{0.02}$]$O_2$.

This work was performed by the financial support of Center for Nanostructured Materials Technology under 21st Century Frontier R&D Programs of the Ministry of Science and Technology.

References

1 J. R. Dahn, U. V. Sacken, and C. A. Mchel, *Solid State Ionics*, **44**, 87 (1990).

2 R. Kanno, H. Kubo, Y. Kawamoto, T. Kamiyama, F. Izumi, Y. Takeda, and M. Takano, *J. Solid State Chem.*, **110**, 216 (1994).

3 T. Ohzuku, A. Ueda, and T. Hirai, *Chem. Express*, **7**, 193 (1992).

4 Y. Gao, M. V. Yakovleva, and W. B. Ebner, *Electrochem. Solid-State Lett.*, **1**, 117 (1998).

5 I. J. Davidson, R. J. Mcllan, J. J. Murray, and J. E. Greedan, *J. Power Sources*, **54**, 232 (1995).

6 L. Croguennec, P. Deniard, and R. Brec, *J. Electrochem. Soc.*, **144**, 3323 (1997).

7 T. Ohzuku and Y. Makimura, *Chem. Lett.*, **2001**, 744.

8 Z. Lu, D. D. MacNeil, and J. R. Dahn, *J. Electrochem. Solid-State Lett.*, **4**, A191 (2001).

9 J.-S. Kim, C. S. Johnson, and M. M. Thackeray, *Electrochem. Commun.*, **4**, 205 (2002).

10 S.-H. Kang and K. Amine, *J. Power Sources*, **119–121**, 150 (2003).

11 Y. Arachi, H. Kobayashi, S. Emura, Y. Nakata, M. Tanaka, and T. Asai, *Chem. Lett.*, **32**, 60 (2003).

12 S. H. Park, S. K. Kang, Y. C. Kang, Y. S. Lee, and Y. K. Sun, *Chem. Lett.*, **32**, 446 (2003).

13 T. Roisnel and J. Rodriguez-Carjaval, "Fullprof Manual," Institute Laue–Langevin, Grenoble (2000).

Published on the web (Advance View) December 1, 2003; DOI 10.1246/cl.2004.2